EPJ Web of Conferences **191**, 08003 (2018) https://doi.org/10.1051/epjconf/201819108003
QUARKS-2018

keV sterile neutrino with large mixing angle is still alive

Anton Chudaykin[1,2,*]

[1]Institute for Nuclear Research of the Russian Academy of Sciences, Moscow 117312, Russia
[2]Moscow Institute of Physics and Technology, Dolgoprudny 141700, Russia

Abstract. We study production of keV scale sterile neutrinos with large mixing with the Standard Model sector [1]. Conventional mechanism of sterile neutrino generation in the early Universe leads to overproduction of the Dark Matter and strong X-ray signal from sterile neutrino decay. It makes anticipated ground-based experiments on direct searches of sterile-active mixing unfeasible. We argue that for models with a hidden sector coupled to the sterile neutrinos cosmological and astrophysical constraints can be significantly alleviated. In developed scenario a phase transition in the hidden sector modifies the standard oscillation picture and leads to significantly larger mixing angles, thus opening new perspectives for future neutrino experiments such as Troitsk ν-mass and KATRIN.
This work was made in collaboration with Fedor Bezrukov and Dmitry Gorbunov.

1 Introduction

Introduction of sterile neutrino is one of the most popular extension of the Standard Model (SM), see [2] for review. In this paper we focus on keV scale sterile neutrinos [3]. Mixing with active neutrino is usually considered to be very small, $\theta^2 \ll 10^{-7}$. Otherwise, it leads to overproduction of the Dark Matter (DM) density today [4, 5]. At the same time, direct laboratory constraints [6–8] reach at most only $\theta^2 \sim 10^{-3}$.

We argue that in the models with a hidden sector production of sterile neutrinos can be strongly suppressed. In the early Universe the most efficient sterile neutrino production via oscillations in plasma refers to temperatures [4, 9]

$$T_{\max} \sim 133\,\mathrm{MeV}\left(\frac{M}{1\,\mathrm{keV}}\right)^{1/3}. \tag{1}$$

Thus, if oscillations are strongly suppressed at this temperature owing to non-trivial dynamics in the hidden sector, the final sterile neutrino abundance will be depleted. In what follows we develop one scenario where oscillations launch at some critical temperature $T_c \ll T_{\max}$.

In section 2 we calculate the sterile neutrino abundance and velocity distribution when oscillations are active, namely at $T \lesssim T_c$. In section 3 we discuss how to suppress sterile neutrino production via oscillations in the early Universe. We focus on the natural idea that this suppression can be efficient in case of different sterile neutrino mass evolution at low and high temperatures. Finally, in section 4 we confront the results obtained in previous

*e-mail: chudy@ms2.inr.ac.ru

sections to different cosmological and astrophysical constraints and find the available region of parameter space.

2 Variable sterile neutrino mass

Generation of sterile neutrinos in the early Universe is usually considered in the following framework, see [4, 5],

$$\mathcal{L} = i\bar{N}\hat{\partial}N + \frac{M}{2}\bar{N^c}N + y_\nu H\bar{\nu}_a N + \text{h.c.}, \tag{2}$$

The Yukawa term in (2) after electroweak transition gives the Dirac mass $m_D = y_\nu\langle H\rangle$ leading to mixing between active and sterile states $\theta \simeq m_D/M$ and active neutrino mass $m = \theta^2 M$. The most interesting parameter region will correspond to sterile neutrino production at temperatures $T \ll 100\,\text{MeV}$, thereby the number of degrees of freedom in plasma g_* can be treated almost constant there. Moreover, we assume that population of active neutrinos is not depleted significantly by convertions to sterile state. It is true for small enough mixing angle θ both above and below the freeze-out of active neutrinos at $T_{\nu,f} \sim 2\,\text{MeV}$. With these assumptions the distribution function of sterile neutrinos $f_N(T, E/T)$ obeys the following Boltzman equation [10]

$$HT\left(\frac{\partial f_N}{\partial T}\right)_{E/T} = \left[\frac{1}{2}\sin^2(2\theta_M)\right]\frac{\Gamma_A}{2}f_A, \tag{3}$$

where the effective mixing angle and rate of weak processess in plasma in assumption of mixing only between electron and sterile neutrinos are given by

$$\sin^2(2\theta_M) = \frac{m_D^2}{m_D^2 + [c\Gamma_A E/M + M/2]^2}, \qquad \Gamma_A \approx 1.27 \times G_F^2 T^4 E, \tag{4}$$

with $c \approx 63$ [11]. The solution of (3) with constant g_* is reduced to

$$\frac{f_N}{f_A} = \frac{2.9}{g_*^{1/2}}\left(\frac{\theta^2}{10^{-6}}\right)\left(\frac{M}{\text{keV}}\right)\int_x^{x_c}\frac{y\,dx'}{(1+y^2x'^2)^2}, \tag{5}$$

where $y \equiv E/T$, $x \equiv 148(T/\,\text{GeV})^3(\,\text{keV}/M)$ with T corresponding to observation time and critical temperature T_c related to the onset of neutrino oscillations. $f_A(y) = 1/(\mathrm{e}^y + 1)$ is the thermal distribution of the active neutrinos and $g_* = 10.75$ is valid just before active neutrino freeze-out. At late times we can put the lower integration limit to $z = 0$ and assuming $T_c \ll 100\,\text{MeV}$ expand (5) for small x_c, arriving at

$$\frac{f_N(y)}{f_A(y)} \simeq 0.13 \times \theta^2\left(\frac{10.75}{g_*}\right)^{1/2}\left(\frac{T_c}{\text{MeV}}\right)^3 \cdot y. \tag{6}$$

This distribution corresponds to a warm spectrum with average momentum $\langle\!\langle p\rangle\!\rangle = 4.1T$. This differs a bit from the usual thermal ratio $\langle\!\langle p\rangle\!\rangle = 3.1T$. Integrating (6) over momentum we obtain the sterile neutrino fraction in the total energy density of the Universe

$$h^2\Omega_N \simeq 4.3 \times \theta^2\left(\frac{10.75}{g_*}\right)^{1/2}\left(\frac{T_c}{\text{MeV}}\right)^3\left(\frac{M}{\text{keV}}\right) \tag{7}$$

which is strongly suppressed for small T_c. In Figure 1 we show our accurate results in case of numerical integration of (3) with temperature dependent g_* and Γ_A following refs. [9, 12].

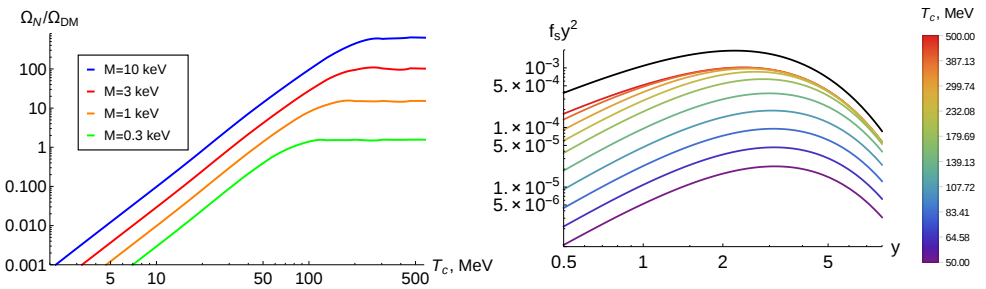

Figure 1. *Left panel:* abundance of the sterile neutrinos produced at $T < T_c$ for several sterile neutrino masses M. *Right panel:* distribution function of sterile neutrinos produced at $T < T_c$ against momentum for one reference sterile neutrino mass $M = 7.1\,\mathrm{keV}$; the top curve shows the thermal Fermi-Dirac distribution for comparison. For both panels $\sin^2(2\theta) = 10^{-6}$ is chosen.

These plots deponstrate excellent aggrement with analytical approach (7) in the interesting temperature range $T_c \ll 100\,\mathrm{MeV}$.

It is worth noting that in case of effectively suppressed oscillations at high temperatures sterile neutrinos with comparably large mixing angle can naturally explain small active neutrino masses within the seesaw type-I mechanism. Indeed, typical values of mixing angle

$$\frac{\theta^2}{10^{-4}} = \frac{1\,\mathrm{keV}}{M}\frac{m}{0.1\,\mathrm{eV}}. \tag{8}$$

are sufficient to explain solar $\sqrt{\delta m^2_{\mathrm{sol}}} \simeq 0.9\times10^{-2}\,\mathrm{eV}$ or atmospheric $\sqrt{\delta m^2_{\mathrm{atm}}} \simeq 0.05\,\mathrm{eV}$ neutrino masses. It is achieveble by T_c in MeV rage when the sterile neutrino contribution (7) is reduced enough $\Omega_N \ll 1$ (see section 4 for details).

3 Phase transition in hidden sector

To suppress neutrino oscillations in the early Universe one should reduce the effective mixing angle in plasma θ_M (4). It can be achieved by introducing a hidden sector coupled to the sterile neutrinos in such a way that sterile neutrinos are either massless or super-heavy at high temperatures. The first option is considered in section 3 whereas the second possibility is examined in the full version of the paper [1]. We consider a model with a rapid change of internal properties of the hidden sector, namely the model with phase transition in the hidden sector.

In this scenario the hidden sector is coupled to active neutrino (SM) sector only via interaction with sterile neutrinos. We also assume that the hidden sector has its own temperature $T_h = \xi T$ which is considerably lower than temperature of the active sector, or $\xi \ll 1$. It means that the hidden sector brings only subdominant contribution to the energy density of the Universe and can be neglected. We introduce the hidden scalar field which interacts with the sterile neutrino through the Yukawa coupling

$$\mathcal{L} = \frac{f}{2}\phi\bar{N}^c N + \mathrm{h.c.}, \tag{9}$$

Thus, the Majorana mass of sterile neutrino after phase transition in the hidden sector attains the addition field-dependent contribution $M \propto f\langle\!\langle\phi\rangle\!\rangle$ where $\langle\!\langle\phi\rangle\!\rangle$ is expectation value of the scalar field.

Desirable evolution of sterile neutrino mass is achieved in the situation when phase transition happens at temperature $T_{h,c} = \xi T_c$. It means that as long as the scalar field is in its symmetric phase

$$\langle\langle\phi\rangle\rangle|_{T_h>\xi T_c} = 0,$$

the sterile neutrino holds massless with high accuracy. After symmetry breaking in the hidden sector the scalar field acquires a non-zero expectation value and sterile neutrino gains the present keV mass

$$\langle\langle\phi\rangle\rangle|_{T_h<\xi T_c} = v_\phi, \qquad M = f v_\phi.$$

If phase trasition is instant, spectrum of sterile neutrinos produced at latter stange is given by (5).

We found that abundance (7) is strongly suppressed with decreasing T_c. Let us find the minimal abundance of sterile neutrinos attainable in the scenario with phase transition. In (6) we assumed that neutrino is exactly massless at T_c. In fact, only Majorana mass is equal to zero at high temperatures. Actually, after electroweak transition neutrino can be approximated as a pure Dirac particle with mass m_D and we expect the admixture of the helicity-suppressed right-handed component at the level of $m_D^2/4p^2 = m_D^2/4y^2T^2$ produced in scatterings. Thus, in addition to (7), there is also an *initial* contribution to the sterile neutrino spectrum

$$\frac{f_{S,\mathrm{in}}}{f_A} \simeq \frac{m_D^2}{4y^2T_c^2} \simeq \frac{0.25\times10^{-6}\theta^2}{y^2}\left(\frac{M}{\mathrm{keV}}\right)^2\left(\frac{\mathrm{MeV}}{T_c}\right)^2, \tag{10}$$

where we exploit $m_D^2 = \theta^2 M^2$ using the present day neutrino mass and mixing angle. Similarily to (7) initial contribution to the spectrum (10) can be easily converted to the present sterile neutrino density

$$h^2\Omega_{N,\mathrm{in}} = \frac{MT_{\nu,0}^3}{(\rho_c/h^2)}\frac{2}{2\pi^2}\int_0^\infty dy\, y^2 f_{S,\mathrm{in}}(y) \approx 10^{-6}\theta^2\left(\frac{M}{\mathrm{keV}}\right)^3\left(\frac{\mathrm{MeV}}{T_c}\right)^2. \tag{11}$$

Comparing initial (11) and late-time (7) contributions we find that they become equal at critical temperature

$$T_{c,\min} \simeq 0.05\,\mathrm{MeV}\left(\frac{M}{\mathrm{keV}}\right)^{2/5}. \tag{12}$$

Thus, the absolute minimum of sterile neutrino abundance produced in the model with instant phase transition can be estimated as

$$h^2\Omega_{N,\min} \simeq h^2\Omega_{N,T<T_C} + h^2\Omega_{N,\mathrm{in}} \simeq 0.9\times10^{-3}\theta^2\left(\frac{M}{\mathrm{keV}}\right)^{11/5}. \tag{13}$$

The final spectrum of sterile neutrinos, in turn, is given by the sum of (6) and (10), $f_N = f_{S,T<T_C} + f_{S,\mathrm{in}}$. The former spectrum is warmer whereas the latter is colder compared to the Fermi-Dirac distribution function. The colder component can presumably weaken constraints on DM velocity distribution. However, as we will see in section 4 this effect appears to be insufficient to extend available parameter space due to a small fraction of initial contribution (11) compared to total DM.

4 Cosmological and astrophysical constraints

We revise cosmological and astrophysical constraints in the scope of production mechanisms suggested in sections 2 and 3 and obtain the parameter region consistent with cosmology.

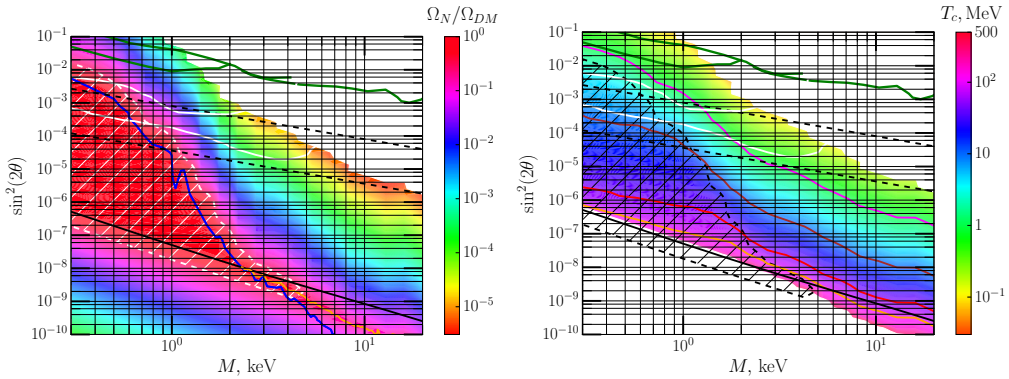

Figure 2. The numerical results for the scenario introduced in section 3. Maximal possible sterile neutrino fraction in the total DM $\Omega_N/\Omega_{\rm DM}$ (left panel) which does not break DM abundace and X-ray constraint, simultaneously, and corresponding phase transition temperature T_c (right panel) shown by color. Green curves on the top of the graphs depict direct bounds from the ground-based neutrino experiments [6–8]. Tho solid white lines correspond to prospective sensitivity of Troitsk ν-mass experiment after two stages of anticipated upgrade [19]. Inclined dashed black lines reflect (8) for two reference masses of active neutrino 0.2 eV and 0.009 eV. Black line corresponds to non-resonant production of $\Omega_N = \Omega_{\rm DM}$. In regions dashed by white (left panel) and black (right panel) inclined lines sterile neutrinos contribute no more than 30% of the whole DM – this fraction of warm component is already prohibited by [18]. White space region in the upper right corner breaks X-ray constraint (14) and, therefore, is unreachable in the model with phase transition. *Left panel:* blue line depicts X-ray constraint (14) in case $\Omega_N = \Omega_{\rm DM}$. Yellow line reflects (15). *Right panel:* orange, red, brown and magenta curves refer to the temperatures of phase transition T_c = 100, 50, 10 and 1 MeV. White region in the lower left corner denotes the area where the phase transition is not required ($T_c \to \infty$).

After that, we confront our results to sensitivities of current and projective ground-based neutrino experiment in keV mass range of sterile neutrinos.

We list three sources of constraints from cosmology and astrophysics. According to the first one the present sterile neutrino abundance cannot exceed the DM fraction, so $\Omega_N \leq \Omega_{\rm DM}$ is required. Second bound comes from a radiative decay mode of sterile neutrino to photon and active neutrino, $N \to \gamma\nu$, leading to the monochromatic line in the spectrum of diffuse X-ray background. This feature can be detected by cosmic X-ray observations. The absence of such signal imposes a strong constraint on mixing angle. We denote this type of constraint as $\theta_{\text{X-ray}}(M)$ assuming that sterile neutrinos compose all the DM today. If sterile neutrinos compose only a fraction of DM, X-ray constraint should be rescaled in the following way

$$\sin^2 2\theta(M) < \frac{\Omega_{\rm DM}}{\Omega_N} \sin^2 2\theta_{\text{X-ray}}(M). \tag{14}$$

Third, if sterile neutrinos compose a significant part of DM bounds from structure formation tests become important. The matter is that the spectrum of DM particles should not be too warm to be consistent with distribution of small satellite galaxies [13], phase space density of galactic DM [14] and analyses of Lyman-α forest [15]. These measurements estimate the average velocity of DM particles putting an upper limit on the level of free-streaming.

In Figure 2 we present the accurate results using numerical solution of (3) and (10) in the scenario of section 3. The plots depict the *maximal* possible sterile neutrino fraction $\Omega_N/\Omega_{\rm DM}$ and *maximal* possible critical temperature (moment of instant phase transition) T_c that satisfy both DM abundance and X-ray constraints.

We shortly list all relevant constraints shown in Fig. 2. Black line depicts $\sin^2 2\theta_{\rm NRP}$ related to non-resonant production of sterile neutrinos with $\Omega_N = \Omega_{\rm DM}$. Blue line denotes X-ray constaints $\theta_{\text{X-ray}}$ in assumption of $\Omega_N = \Omega_{\rm DM}$. In region $\theta_{\text{X-ray}} < \theta_{\rm NRP}$ the actual X-ray constraint is shown by orange line defined by

$$\theta^2_{\max\,\text{X-ray}}(M) = \sqrt{\theta^2_{\text{X-ray}}(M)\theta^2_{\rm NRP}(M)}. \tag{15}$$

Indeed, according to Fig. 2 amount of sterile neutrinos poduced in this region (below non-resonant production black line) is small and one should adopt the usual X-ray constraint for the case $\Omega_N < \Omega_{\rm DM}$.

In the region below both black and orange lines in Fig. 2 the phase transition is not needed since sterile neutrinos compose only a fraction of DM and satisfy X-ray constraint (14) itself. The same concerns the region between blue and orange lines in Fig. 2. White space in the upper right corner of Fig. 2 denotes the forbidden region where suppression of oscillations is not sufficient to satisfy X-ray constraint (14) in the model with phase transition.

In the triangular region at the left of Fig. 2 limited by black and blue lines sterile neutrinos can compose all the DM, $\Omega_N = \Omega_{\rm DM}$, solely by reducing T_c. However, this parameter region is in strong conflict with structure formation tests. Indeed, conservative bounds in case of non-resonantly produced DM are $m_{\rm NRP} > 8\,\text{keV}$ from Lyman-α [16] and $m_{\rm NRP} > 5.7\,\text{keV}$ [17] from phase space density. In case of warm spectrum (6) these mass bounds are rescaled with a help of

$$m_{\rm NRP} = \frac{\langle\!\langle p \rangle\!\rangle|_{f_A}}{\langle\!\langle p \rangle\!\rangle|_{f_N}} M = \frac{3.1}{4.1} M, \tag{16}$$

to the followings $M > 11\,\text{keV}$ and $M > 8\,\text{keV}$, respectivily. Apparently, structure formation constraints would be less stringent if sterile neutrinos composed only a part of DM. Current investigation in this field had just begun and, therefore, are rather inacurate so far. For this reason we simply dashed the prohibited region by white (left plot) and black (right plot) inclined lines in Fig. 2 where sterile neutrinos contribute more than 30% of total DM. This region is prohibited because sterile neutrinos are too warm according to [18].

As seen from Fig. 2 in the model of section 3 for special sterile neutrino mass range the mixing angle can reach even direct constraints from the current laboratory experiments (green solid lines) adopting $T_c > T_{c,min}$.

We point out that in our analysis sterile neutrino mixes only with electronic neutrino. However, the upper bound of available region (upper edge of colour area in Fig. 2) does not depend on particular neutrino flavour. Indeed, after electron decoupling the interaction rate of active neutrino with plasma is the same for all flavours.

Finally, the model of section 3 predicts the significant extension of available parameter region consistent with all cosmological and astrophysical constraints. In some range of sterile neutrino masses active-sterile mixing can reach even the direct bounds from current particle physics experiments. Mixing at the level of (8) can also explain small active neutrino masses in the scope of the suggested model. Latter possibility can be tested by presently developing ground-based experiments, see [19] for details.

5 Conclusion

To conclude, we develop a new mechanism of sterile neutrino production in the early Universe. Introducing the hidden sector with non-trivial dynamics – phase transition – we effectively suppress neutrino conversions by making sterile neutrino merely massless at high

temperatures. Hence, the active-sterile neutrino mixing can be significantly larger as compared to the standard oscillation picture. In some range of sterile neutrino mass one can reach the bounds from the direct searches.

Remarkably, in the suggested scenario one can directly probe the mixing which naturally explains small active neutrino masses within the seesaw type-I mechanism. Thus, the forthcoming ground-based experiments will be able to exclude this possibility in the future.

All possible scenarios are not limited by this one considered in the paper. For instance, a frozen classical field can make sterile neutrino, conversely, super-heavy in the early Universe; it disables neutrino oscillations at high temperatures kinematically. This and others scenarios are outlined in the full version of this paper [1].

The works is supported by the RSF grant 17-12-01547.

References

[1] F. Bezrukov, A. Chudaykin and D. Gorbunov, JCAP **1706**, no. 06, 051 (2017).
[2] K. N. Abazajian *et al.*, arXiv:1204.5379 [hep-ph].
[3] M. Drewes *et al.*, JCAP **1701**, no. 01, 025 (2017).
[4] S. Dodelson and L. M. Widrow, Phys. Rev. Lett. **72**, 17 (1994).
[5] A. D. Dolgov, Phys. Rept. **370**, 333 (2002).
[6] K. H. Hiddemann, H. Daniel and O. Schwentker, J. Phys. G **21**, 639 (1995).
[7] E. Holzschuh, W. Kundig, L. Palermo, H. Stussi and P. Wenk, Phys. Lett. B **451**, 247 (1999).
[8] J. N. Abdurashitov *et al.*, Pisma Zh. Eksp. Teor. Fiz. **105**, no. 12, 723 (2017) [JETP Lett. **105**, no. 12, 753 (2017)].
[9] K. Abazajian, G. M. Fuller and M. Patel, Phys. Rev. D **64**, 023501 (2001).
[10] K. Enqvist, K. Kainulainen and M. J. Thomson, Nucl. Phys. B **373**, 498 (1992).
[11] T. Asaka, M. Laine and M. Shaposhnikov, JHEP **0701**, 091 (2007).
[12] J. Ghiglieri and M. Laine, JHEP **1511**, 171 (2015).
[13] P. Bode, J. P. Ostriker and N. Turok, Astrophys. J. **556**, 93 (2001).
[14] S. Tremaine and J. E. Gunn, Phys. Rev. Lett. **42**, 407 (1979).
[15] V. K. Narayanan, D. N. Spergel, R. Dave and C. P. Ma, Astrophys. J. **543**, L103 (2000).
[16] A. Boyarsky, J. Lesgourgues, O. Ruchayskiy and M. Viel, JCAP **0905**, 012 (2009).
[17] D. Gorbunov, A. Khmelnitsky and V. Rubakov, JCAP **0810**, 041 (2008).
[18] R. Diamanti, S. Ando, S. Gariazzo, O. Mena and C. Weniger, JCAP **1706**, no. 06, 008 (2017).
[19] D. N. Abdurashitov *et al.*. JINST **10**, no. 10, T10005 (2015).